PORTLAND PRESS

Research Article

α-Helix stabilization by co-operative side chain charge-reinforced interactions to phosphoserine in a basic kinase-substrate motif

Matthew Batchelor[1,2], Robert S. Dawber[1,3], Andrew J. Wilson[1,3] and ⓘ Richard Bayliss[1,2]

[1]Astbury Centre for Structural Molecular Biology, University of Leeds, Woodhouse Lane, Leeds LS2 9JT, U.K.; [2]School of Molecular and Cellular Biology, University of Leeds, Woodhouse Lane, Leeds LS2 9JT, U.K.; [3]School of Chemistry, University of Leeds, Woodhouse Lane, Leeds LS2 9JT, U.K.

Correspondence: Richard Bayliss (r.w.bayliss@leeds.ac.uk) or Andrew J. Wilson (a.j.wilson@leeds.ac.uk)

OPEN ACCESS

How cellular functions are regulated through protein phosphorylation events that promote or inhibit protein–protein interactions (PPIs) is key to understanding regulatory molecular mechanisms. Whilst phosphorylation can orthosterically or allosterically influence protein recognition, phospho-driven changes in the conformation of recognition motifs are less well explored. We recently discovered that clathrin heavy chain recognizes phosphorylated TACC3 through a helical motif that, in the unphosphorylated protein, is disordered. However, it was unclear whether and how phosphorylation could stabilize a helix in a broader context. In the current manuscript, we address this challenge using poly-Ala-based model peptides and a suite of circular dichroism and nuclear magnetic resonance spectroscopies. We show that phosphorylation of a Ser residue stabilizes the α-helix in the context of an $Arg_{(i-3)}pSer_i Lys_{(i+4)}$ triad through charge-reinforced side chain interactions with positive co-operativity, whilst phosphorylation of Thr induces an opposing response. This is significant as it may represent a general method for control of PPIs by phosphorylation; basic kinase-substrate motifs are common with 55 human protein kinases recognizing an Arg at a position −3 from the phosphorylated Ser, whilst the $Arg_{(i-3)}Ser_i Lys_{(i+4)}$ is a motif found in over 2000 human proteins.

Introduction

The determinants of α-helix stability are key in understanding the formation and strength of α-helix mediated protein–protein interactions (PPIs) [1], and therefore in enabling peptide drug-discovery [2,3]. Prior studies established helix propensities of individual amino acids [4,5], the role of helix capping [6,7] and effects of interaction between side chains [8–11]; however, the role of phosphorylation is less well explored.

Classically, phosphorylation occurs within solvent-exposed loops or disordered regions [12]. Such phosphorylation events play a regulatory role in the PPI network of substrate proteins; primed with a new highly charged phosphate group as a recognition feature, such regions can bind to a different protein to activate or deactivate a subsequent cellular process [13]. More recently, phosphorylation has been shown to affect secondary/tertiary structure, e.g. the intrinsically disordered 4E-BP2 undergoes a disorder-to-helix transition upon binding to eIF4E, but on multisite phosphorylation, folds instead into a four-stranded β-domain [14]. Ser phosphorylation has been shown to increase helicity in model peptides [15], notably at the N-terminus [16,17], a feature exploited in design of phosphorylation-stabilized tertiary helix structures [18,19]. Secondary structure has also been shown to be destabilized by phosphorylation [20,21] with internal phosphorylation of Thr and Ser residues helix destabilizing [15–17]. Herein we describe the effects of phosphorylation on helix stability using model poly-Ala-based peptides, into which we grafted a motif inspired by studies on the Aurora A/TACC3/CHC pathway, an unusual example of a PPI centred on a phosphorylated helix [22].
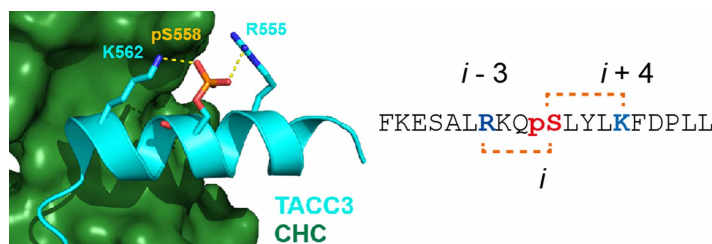
Figure 1. TACC3 structure in the TACC3/CHC complex.

X-ray crystal structure for the TACC3/CHC interaction (PDB ID: 5ODS; TACC3 cyan, CHC forest green), together with the TACC3 sequence; the Arg$_{(i−3)}$pSer$_i$ Lys$_{(i+4)}$ motif is highlighted with side chains shown as sticks.

Aurora A-mediated phosphorylation of TACC3, a member of the transforming acidic coiled coil (TACC) family of centrosomal and microtubule-associated proteins, promotes complex formation with clathrin heavy chain (CHC) protein resulting in molecular 'bridges' across parallel microtubules to ensure accurate chromosome alignment and segregation during mitosis. The TACC3/CHC complex is α-helix mediated [22]; the TACC3 residue phosphorylated by Aurora A, Ser558, is in a basic kinase-substrate motif, flanked by basic Arg555 and Lys562 residues in $i − 3$ and $i + 4$ positions rendering them suitably placed to stabilize helicity via interactions with the phosphate (Figure 1). The TACC3-inspired Arg$_{(i−3)}$pSer$_i$ Lys$_{(i+4)}$ motif was grafted into a well-studied poly-Ala-based model peptide [23,24]. Poly-Ala peptides are good models due to their intrinsic α-helix-forming propensity; sequence modifications can be related to the introduction/deletion of potential interactions between side chains [9,25]. Peptides were designed to investigate the α-helix stabilizing influence of phosphate salt bridging. The phosphorylation state was altered, Arg and Lys side chains were systematically moved in and out of pSer registry, and the effect of substitution of Ser for Thr was studied (Scheme 1).

Results

Basic residues in flanking positions enhance the helicity of peptides incorporating a pSer residue

A range of peptides (**1–10**, Table 1) were designed and prepared using solid phase synthesis as N-terminal acetamides and C-terminal amides (see Supplementary Information for analytical characterization data). The relative helical propensity for each of the peptides was established using far UV circular dichroism (CD) spectroscopy [26]. Figure 2a compares the CD spectrum of the phosphorylated and unphosphorylated peptides **1** and **2**. **1** exhibits a CD profile characteristic of an α-helix with negative bands at 222 and 208 nm, and a positive band at ∼190 nm (Figure 2a, see Supplementary Figure S1 for data demonstrating spectra are concentration independent). For peptide **2**, reduced helicity is indicated from smaller bands at 222 and 190 nm, and a shift of the peak at 208 nm to lower wavelength. Estimation of the % helicity using the mean residue ellipticity (MRE) value at 222 nm gave 29% for **1** and 22% for **2** (Table 1), indicating that phosphorylation enhances helicity with $i − 3$ Arg and $i + 4$ Lys
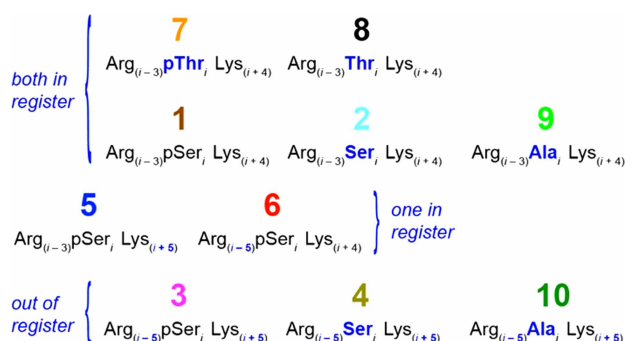
Scheme 1. The 10 peptides used in the study are arranged to highlight their relationships. Differences in sequence from the Arg$_{(i−3)}$pSer$_i$ Lys$_{(i+4)}$ motif of peptide **1** are highlighted in blue, bold text. Peptides are grouped according to whether the positively-charged residues are in or out of register with their positions in peptide **1**.

Table 1 Sequences, MRE_{222} data, helicity estimates and free energies values calculated for poly-Ala model peptides 1–10

Peptide	Sequence[1]	MRE_{222}[2] (deg cm^2 dmol^{-1})	Estimate % helix	N	ΔG_x[3] (kJ mol^{-1})	$\Delta\Delta G$ wrt unphos[4] (kJ mol^{-1})	$\Delta\Delta G$ wrt 3[5] (kJ mol^{-1})	$\Delta\Delta G$ wrt Ala[6] (kJ mol^{-1})
1	Ac-AAQAAARQApSAAQKAY-NH$_2$	−9600 ± 600	29 ± 2	7	2.1	−0.8	−4.0	1.0
2	Ac-AAQAAARQA SAAQKAY-NH$_2$	−7400 ± 500	22 ± 1	7	2.9	—	−3.2	1.8
3	Ac-AAQARAAQApSAAQAKY-NH$_2$	−1900 ± 100	7 ± 1	6	6.1	3.1	—	5.1
4	Ac-AAQARAAQA SAAQAKY-NH$_2$	−7300 ± 400	22 ± 1	4	2.9	—	−3.1	1.9
5	Ac-AAQAAARQApSAAQAKY-NH$_2$	−4000 ± 200	13 ± 1	5	4.5		−1.6	
6	Ac-AAQARAAQApSAAQKAY-NH$_2$	−4100 ± 300	13 ± 1	6	4.4		−1.7	
7	Ac-AAQAAARQApTAAQKAY-NH$_2$	−230 ± 40	1.8 ± 0.4	4	9.2	5.7		8.1
8	Ac-AAQAAARQA TAAQKAY-NH$_2$	−5900 ± 200	18 ± 1	4	3.5	—		2.4
9	Ac-AAQAAARQA AAAQKAY-NH$_2$	−13000 ± 700	38 ± 2	4	1.1			—
10	Ac-AAQARAAQA AAAQKAY-NH$_2$	−13300 ± 500	39 ± 2	6	1.0			—

[1]Residues with positive charges are highlighted in blue; residues with negative charges are highlighted in red;
[2]% Helicity values shown were calculated based on MRE_{222} values recorded at 5°C (see Experimental section);
[3]ΔG_x values are estimates of the Gibbs free energy change for the folded peptides in solution relative to their unfolded states;
[4]$\Delta\Delta G$ values are the change in the Gibbs free energy change from differences in ΔG_x values, here given relative to the unphosphorylated version of the peptide (**2**, **4** or **8**);
[5]$\Delta\Delta G$ values relative to the least helical pSer-containing peptide **3**;
[6]$\Delta\Delta G$ values relative to the Ala-control peptide (**9** or **10**) with the same R and K spacing. N is the number of independent measurements.

basic side chains. Variant pSer to Ala-control peptides were more helical as would be expected given the increased helical propensity of Ala (peptides **9** and **10**, Table 1, Supplementary Figure S2) [4]. The variation in MRE_{222} with temperature indicated a broad transition from part-helical to coil structures and weak folding co-operativity as expected for short peptides of this length (Supplementary Figure S3). At ~70°C, all peptides converged at ~4000 deg cm^2 dmol^{-1} indicating complete loss in helical content at these temperatures.

The effect on peptide helicity of moving Arg and Lys out of helical-registry was explored (Figure 2b). In a peptide where no helix compatible side chain interactions with the phosphate are possible, α-helicity was lowest (**3**, 7%), as expected given the propensity of pSer to be destabilizing in the centre of an α-helix [17]. Indeed, the unphosphorylated version (**4**) has higher helicity, matching that of peptide **2** (Table 1, Supplementary Figure S2). The similarity of the helicity of peptides **4** and **2** (and peptides **9** and **10**, Table 1, Supplementary Figure S2) indicates that the position of Lys and Arg has little effect on the overall helicity when there is no phosphoryl group with which to interact. Having an Arg residue $i − 3$ or Lys residue $i + 4$ to the pSer increased the α-helix-forming propensity (**5** and **6**, both 13%). CD analyses on the pThr-containing peptide **7** indicated low helicity (2%) whereas the Thr analogue elicited higher helicity (**8**, 18%) similar to unphosphorylated Ser peptide **2** (Figure 2c). The additional methyl group in pThr compared with pSer will likely reduce the helix compatible side chain dihedral angle pairings that allow the phosphoryl group to interact with flanking basic residues. More generally, pThr shows a proclivity to adopt a compact conformation due to intraresidue phosphate–amide hydrogen bonding, inter-residue n → π* interactions between consecutive carbonyls, and an eclipsed conformation of the C–OP bond arising from an n → σ* interaction. Such a conformation is incompatible with a helical conformation and is evidently not countered by the benefit of side chain hydrogen bonding as for pSer (peptide **1**) [27].

Side chain interactions that enhance pSer peptide helicity are pH dependent and positively cooperative

The effect of pH on helicity for peptide **1** provided useful insights into the contribution of charge-based interactions between side chains (Figure 3). Protonating the phosphate by reducing the pH below the pK_a of PO_3^{2-} (pH < 5 forming singly charged PO_3H^-) or deprotonating the Lys or Arg groups at high pH would be anticipated to reduce or eliminate charge-reinforced interactions between side chains. The estimated helicity of peptide **1** at low pH is ~16% and at high pH is ~6%, similar values to those of peptide **5/6** (with a single
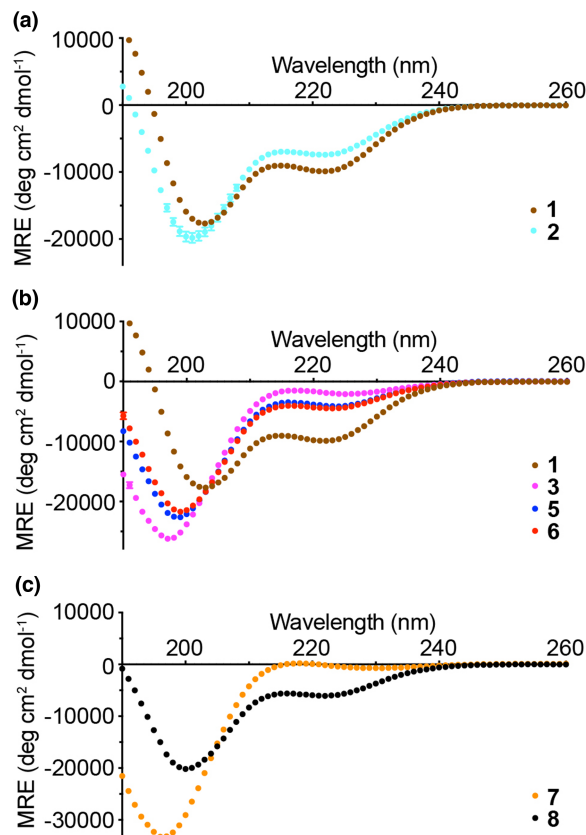
Figure 2. CD spectroscopy for model peptides.

(**a**) CD spectra for peptides **1–2** showing the effect of phosphorylation on the Arg$_{(i-3)}$Ser$_i$ Lys$_{(i+4)}$ motif. (**b**) CD spectra for **1, 3, 5** and **6** illustrating the effect of moving one or two basic groups out of 'helical-registry' with the pSer. (**c**) CD spectra for peptides **7–8** showing the effect of phosphorylation on the Arg$_{(i-3)}$Thr$_i$ Lys$_{(i+4)}$ motif. Experiments were carried out at 5°C in CD buffer (10 mM NaCl, 1 mM sodium phosphate, 1 mM sodium borate and 1 mM sodium citrate) at pH 7. Peptide concentrations were in the range 50–100 μM.
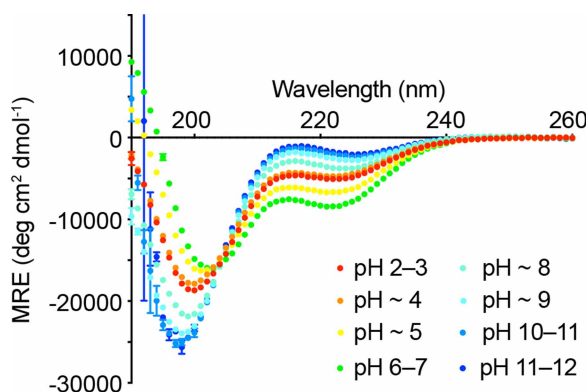

Figure 3. The effect of pH on the helicity of peptide 1.

Low and high pH reduce peptide **1** helicity indicating that charge-reinforced side chain interactions stabilize the helix. Experiments were carried out at 5°C in CD buffer (10 mM NaCl, 1 mM sodium phosphate, 1 mM sodium borate and 1 mM sodium citrate). Peptide concentrations were in the range 50–100 μM. The pH was altered by the addition of small amounts of 0.1 M HCl or 0.05 M NaOH, with volume changes factored-in to concentration and MRE calculations.

potential X^+–PO_3^{2-} interaction) and peptide **3** (no interaction), respectively. For comparison, the more limited effect of changing pH on peptide helicity for other selected peptides is shown in Supplementary Figure S4.

We used the measured % helicity values to estimate the Gibbs free energy change of the α-helical peptides in solution relative to their unfolded states, ΔG (Table 1) [11]. This allowed us to make quantitative estimates of the change in the Gibbs free energy change for helix formation, $\Delta\Delta G$, associated with phosphorylation or formation of charge-reinforced side chain interactions involving the phosphate. $\Delta\Delta G$ values measured relative to unphosphorylated peptides (Table 1) show that phosphorylation can have a wide-ranging influence, being beneficial (-0.8 kJ mol^{-1}) in the case of $Arg_{(i-3)}Ser_i Lys_{(i+4)}$, highly destabilizing (5.7 kJ mol^{-1}) in the case of $Arg_{(i-3)}Thr_i Lys_{(i+4)}$ and moderately destabilizing for $Arg_{(i-5)}Ser_i Lys_{(i+5)}$ where no side chain interactions are possible (3.1 kJ mol^{-1}). By relating the ΔG of **5** to that of **3** (Table 1), the formation of such an interaction between the phosphate group and $i-3$ Arg side chain has a $\Delta\Delta G$ of -1.6 kJ mol^{-1}. Comparison of ΔG values for **6** and **3** show that potential interaction between the phosphate and the $i+4$ Lys side chain has a similar $\Delta\Delta G$ (-1.7 kJ mol^{-1}). These values are in agreement with typical values for the formation of charge-reinforced interactions between side chains in helices [28,29], e.g. Glu–Lys ($i, i\pm 3$ or $i, i\pm 4$) interactions under similar conditions gave rise to $\Delta\Delta G$ values of 1.2–1.7 kJ mol^{-1} [29]. For both **5** and **6**, the ability to form interactions between side chains is insufficient to offset the destabilizing effect of introducing a pSer in the middle of the helical sequence (**4** vs. **3**, $\Delta\Delta G = -3.1$ kJ mol^{-1}) [16]. In contrast, **1**, where both interactions can form, would be expected to have a reported $\Delta\Delta G$ (relative to **3**) of ~ -3.3 kJ mol^{-1} if the contributions were additive (only marginally higher than the $\Delta\Delta G$ for **2**). However, with a $\Delta\Delta G$ of -4.0 kJ mol^{-1}, this indicates that the effects of two charge-reinforced interactions with phosphate are positively cooperative.

Calculating $\Delta\Delta G$ values relative to Ala-control peptides (Table 1) shows that the replacement of Ala10 with Ser decreases helix stability by 1.8–1.9 kJ mol^{-1} (**2** and **4**). Phosphorylation to pSer rescues approximately half of the original stabilizing energy (0.8 kJ mol^{-1}) when both positively charged residues are in register (compare **1** and **2**) or further destabilizes the helix by 3.2 kJ mol^{-1} when they are out of register (compare **3** and **4**).

NMR chemical shifts show increased helicity in pSer peptides with in-helical-range basic residues

To provide additional structural insight to complement the CD analyses, a suite of four NMR spectra was recorded for each peptide to assign ^1H, ^{13}C and ^{15}N resonances. Residue assignments in a ^1H–^{15}N HMQC
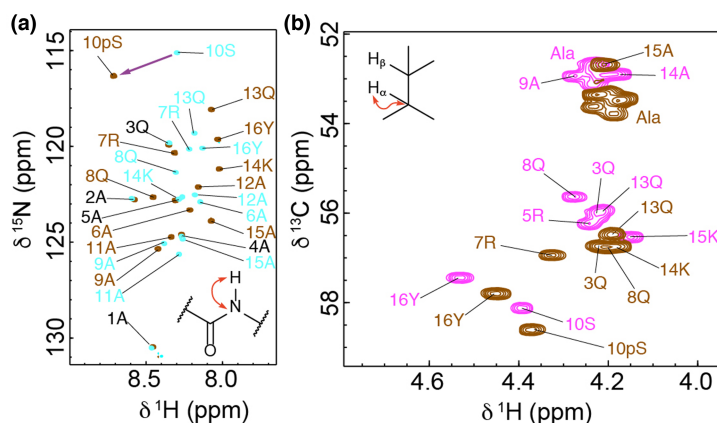

Figure 4. NMR spectroscopy of peptides.
(**a**) A comparison of part of the ^1H–^{15}N HMQC spectra for peptides **1** (brown) and **2** (blue), showing the effect of phosphorylation on main-chain HN peaks of the $Arg_{(i-3)}Ser_i Lys_{(i+4)}$ motif peptide; (**b**) A comparison of regions of ^1H–^{13}C HSQC spectra for peptides **1** (brown) and **3** (magenta) showing Arg Hα-Cα correlations. These spectra highlight the difference between a phospho-peptide that is capable (**1**) or incapable (**3**) of forming inter-turn interactions between the phosphate group and neighbouring basic residues (Arg and Lys). Spectra were recorded on a 600-MHz Bruker Avance spectrometer equipped with a quadruple resonance QCI-P cryoprobe, or a 950-MHz Bruker Ascend Aeon spectrometer equipped with a 5 mm TXO cryoprobe. Experiments were performed in CD buffer (10 mM NaCl, 1 mM sodium phosphate, 1 mM sodium borate, and 1 mM sodium citrate, pH 6.5–7) at 5°C. Peptide concentrations were in the range 0.5–1.0 mM.

spectrum were achieved using a combination of ^{1}H–^{1}H TOCSY/NOESY spectra, informed by a ^{1}H–^{13}C HSQC spectrum and systematic peak position shifts between spectra for different peptides. Natural abundance ^{1}H–^{15}N HMQC spectra for peptides **1** and **2** are shown in Figure 4a; phosphorylation leaves H–N peak positions for residues 1–5 largely unaffected whilst a characteristic downfield shift is observed for the backbone H–N of pSer with respect to Ser as marked by the purple arrow [30]. Neighbouring residues also exhibit shifts with the phosphorylated peptide **1** showing greater peak dispersion than the unphosphorylated peptide **2**, suggesting increased secondary structure content. Patterns in Cα shifts also provide a useful guide to local secondary structure. Figure 4b shows the Hα–Cα region of ^{1}H–^{13}C HSQC spectra for two examples, peptide **1** and peptide **3** with Arg and Lys in- and out-of-helical-range, respectively. Systematic downfield Cα shifts and upfield Hα shifts observed for peptide **1** compared with peptide **3** indicate increased helical content. To account for
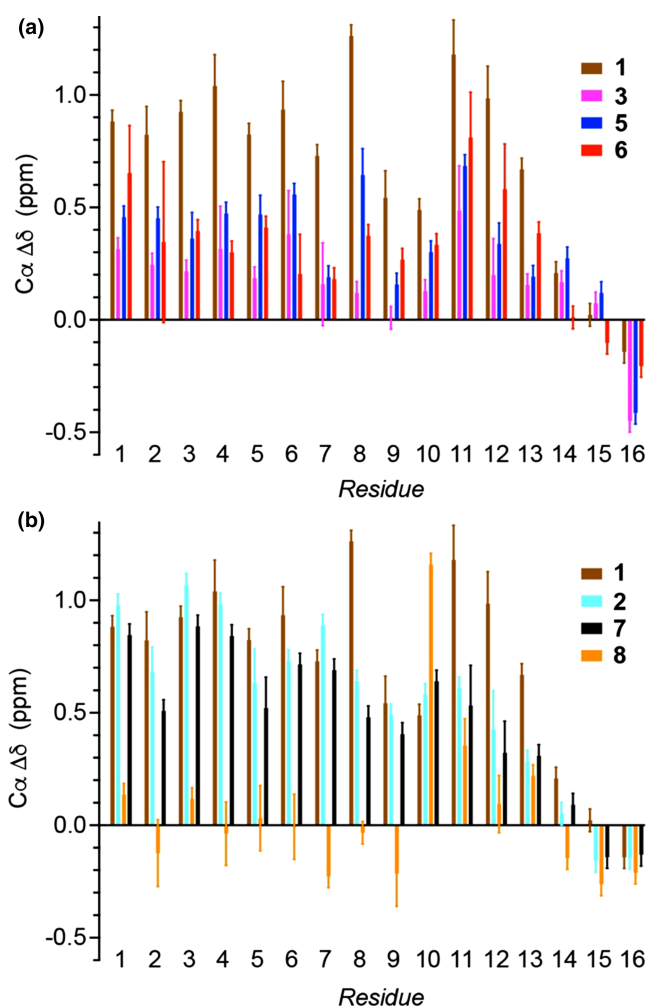

Figure 5. Residue-specific Cα secondary shifts at 5°C and pH 6.5–7.
Secondary shift values are plotted for each residue for (**a**) peptides **1**, **3**, **5** and **6**, showing the effect of changing the position of the basic residues, and (**b**) peptides **1**, **2**, **7** and **8**, showing the effect of phosphorylation. Error bars represent the range in possible shift measurements from ^{1}H–^{13}C HSQC spectra — particularly important for the overlapping Ala Hα–Cα peaks. Shifts recorded from clean/distinct peaks are shown with a baseline error of 0.05 ppm (related to the peak width). Secondary shifts from spectra for peptides **1** and **7** recorded at pH values between 6 and 7.5, showed no significant variation. Spectra were recorded on a 600-MHz Bruker Avance spectrometer equipped with a quadruple resonance QCI-P cryoprobe, or a 950-MHz Bruker Ascend Aeon spectrometer equipped with a 5 mm TXO cryoprobe. Experiments were performed in CD buffer (10 mM NaCl, 1 mM sodium phosphate, 1 mM sodium borate and 1 mM sodium citrate). The pH was altered by the addition of small amounts of 0.1 M HCl or 0.05 M NaOH. Peptide concentrations were in the range 0.5–1.0 mM.

changes in sequence between peptides, secondary shifts ($\Delta\delta$) (observed shifts (δ) — expected shifts for that residue in a random coil conformation (δ_{RC})) [31–33] were calculated using random coil values that were recently updated to include values for phosphorylated residues (Figure 5) [34]. Plots show the effect of altering the position of the basic residues (Figure 5a) and the effect of phosphorylation (Figure 5b). Data for control Ala peptides **9** and **10**, as well as unphosphorylated peptide **4** are shown in Supplementary Figure S5. These data largely mirror the CD data and show the weighting of the more helical residues towards the N-terminus. It was noted that the pThr Cα secondary shift values are higher than expected for a residue in a random coil configuration, indicating that pThr occupies an arrangement unlike that in the QQpTQQ peptide used to generate the values [34]. Example spectra showing the expected effect of pH on pSer and pThr Hα–Cα correlations are given in Supplementary Figure S6.

Interaction effects shown through specific side chain resonance analyses

Confirmation of intra-helix side chain interactions was obtained using additional NMR experiments focussed on side chain resonances. Performing experiments at a low temperature of 5°C maximizes the helical content and when coupled with use of low pH (below pH 7) also reduces proton exchange enough for Arg Hϵ–Nϵ side chain groups to be visible in ^{1}H–^{15}N HMQC spectra [35]. Each peptide has a single Arg residue resulting in a single Hϵ–Nϵ correlation (Figure 6a). The Arg Hϵ shift appears at ~7.25 ppm for all peptides with the exception of peptide **5** (7.5 ppm) and peptide **1** (7.8 ppm), both of which have Arg in the $i-3$ position relative to the phosphorylated residue — a position suitable for interactions between side chains across a helical turn — and have been shown to be helical. The magnitude of the downfield shift with respect to peptides that have no potential to form such interactions correlates with the overall helicity of the peptide and thus peptide **1** has the largest downfield shift, peptide **5** has an intermediate value and peptide **7** is unmoved. The Hϵ shift for peptide **1** is similar to those reported for Arg residues in a single-α-helix domain that had three potential Glu salt bridge partners (7.7–7.9 ppm) [36]. In line with the CD analyses, on decreasing pH, the Hϵ resonance in peptide **1** experiences an upfield shift indicating a loss of interaction as the phosphate starts to become protonated (Figure 6b), whereas the Hϵ–Nϵ correlation in peptide **3** does not change (Figure 6c). Under the standard conditions ($T = 5$°C, pH 6.5–7) the Arg Hη–Nη and Lys Hζ–Nζ were not visible in ^{1}H–^{15}N HMQC spectra, although at lower pH [37], the Lys Hζ–Nζ correlation could be observed and the Hζ resonance for **1** was slightly downfield in comparison to **3** (Figure 6d). In addition, ^{1}H–^{13}C HSQC and ^{1}H–^{1}H TOCSY spectra revealed that the diastereotopic Arg Hδ protons were resolved in a pH-dependent manner for **1** alone, indicating a more restricted side chain conformation for this peptide (Figure 6e–f). For comparison, ^{1}H–^{1}H TOCSY spectra showing Arg Hϵ–Hδ correlations for peptides **3**, **5**, **6** and **7** are given in Supplementary Figure S7. The two Arg Hγ resonances for **1** also become non-equivalent on increasing the pH (Supplementary Figure S8). However, this effect appears to be related to the helicity of the peptide, rather than interaction with the phosphoryl group, since distinct Hγ resonances are also observed for helical, nonphosphorylated peptides **2** and **9**.

1D ^{31}P spectra provided further evidence for differences between peptides in phosphate shielding and altered pSer/pThr side chain dihedral propensities. ^{31}P NMR spectra of phospho-peptides contain two peaks: one from the 1 mM free phosphate in the buffer and one from pSer/pThr (Figure 7). pSer ^{31}P resonances appear as a triplet (sometimes unresolved) due to $^3J_{PH}$ coupling to the two β protons, pThr ^{31}P resonances appear as a doublet through coupling to the single β proton. These spectra are highly sensitive to changes in pH. The buffer phosphate peak provides a guide to sample pH through calibration of peak position using standard CD buffer samples at pH 5, 6, 7 and 8. At low pH (pH 5, Figure 7a), the doublet from peptide **7** appears upfield of the buffer phosphate peak, whereas the triplets from the pSer-containing peptides **1**, **3**, **5** and **6** appear downfield. The ordering of the peptide ^{31}P chemical shifts ($\mathbf{7 < 3 < 6 \sim 5 < 1}$) at pH 5 follows the helicity. This suggests a de-shielding effect as the phosphate is involved in interactions with more neighbouring basic groups, although the (likely related) effect of altered PO_3^{2-}/PO_3H^- equilibrium could be a more significant factor. At high pH (pH ~ 8, Figure 7b) the peak positions are all downfield of the buffer phosphate and they are closer together in chemical shift ($\mathbf{7 < 1 < 3 \sim 5 \sim 6}$). The fine structure of the peaks is clearer at pH 8 allowing the $^3J_{PH}$ coupling constants to be measured (Figure 7c). There is an inverse correlation between peptide helicity and $^3J_{PH}$, with non-helical peptide **7** having the highest $^3J_{PH}$ (9 Hz) and peptide **1** having the lowest (5.3 Hz). These values match very well with those found by Pandey et al. [27] for pThr- and pSer-containing peptides; the high value for peptide **7** suggests a well-defined P–O–C–H dihedral and ordered pThr side chain, whereas the lower values for peptides **3**, **5** and **1** are consistent with a greater degree of pSer side chain freedom. The
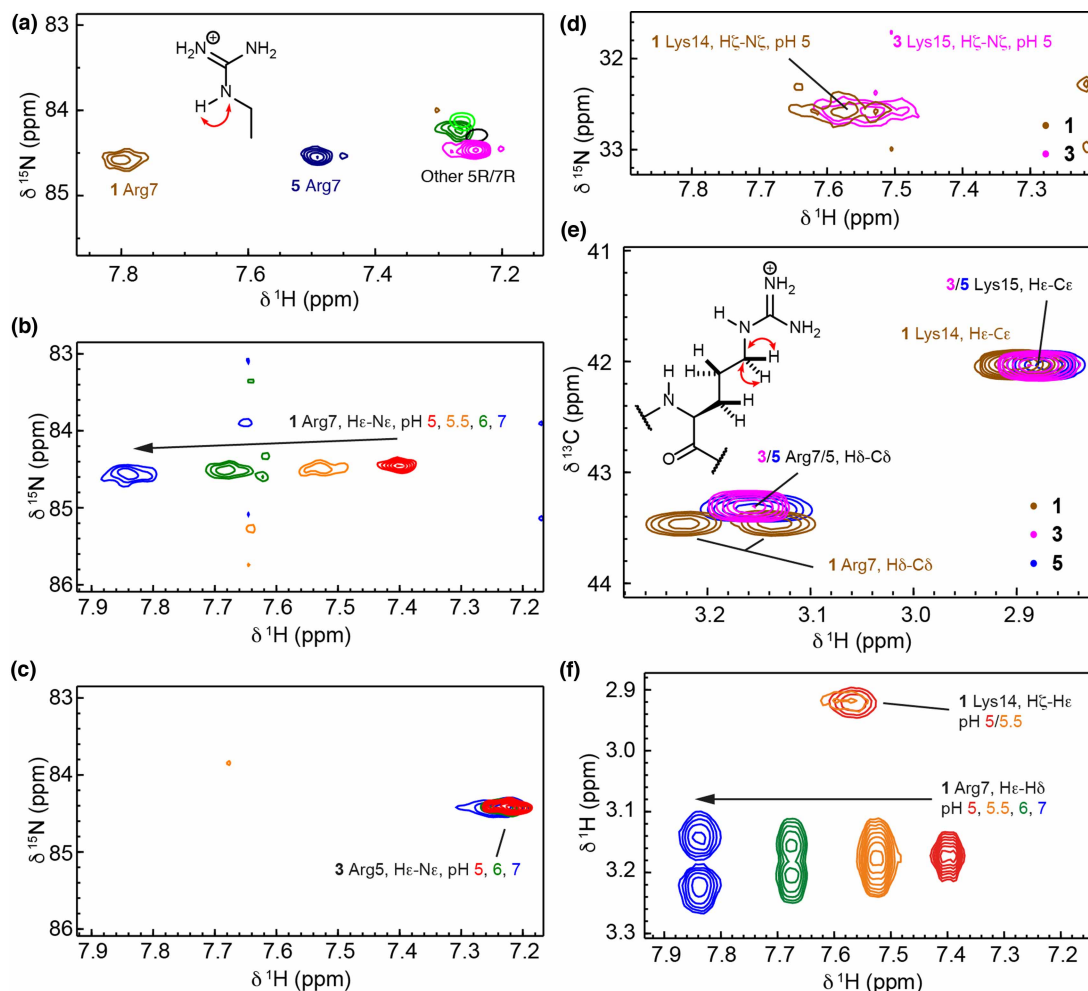
Figure 6. NMR correlation spectroscopy to investigate side chain interactions.
(**a**) The region of the ¹H–¹⁵N HMQC spectra showing Arg Hε–Nε correlations at pH 7 for various peptides that have Arg at position 5 or 7. (**b,c**) The region of the ¹H–¹⁵N HMQC spectra showing pH-dependent chemical shifts in the Arg Hε–Nε correlation for peptides **1** (**b**) and **3** (**c**). (**d**) The region of the ¹H–¹⁵N HMQC spectra showing a small chemical shift difference in the Lys Hζ–Nζ correlations for peptides **1** and **3** at pH 5. (**e**) The region of ¹H–¹³C HSQC spectra for peptides **1**, **3** and **5**, pH 7, showing Arg Hδ–Cδ correlations and Lys Hε–Cε correlations. Note the non-equivalence of the two Hδ for peptide **1** only. (**f**) The region of ¹H–¹H TOCSY spectra for peptides **1**, **3** and **5** at pH values 5–7, showing Arg Hε–Hδ and Lys Hζ–Hε correlations. Again, the two Hδ for peptide **1** are not equivalent at high pH. Spectra were recorded on a 600-MHz Bruker Avance spectrometer equipped with a quadruple resonance QCI-P cryoprobe at 5°C in CD buffer (10 mM NaCl, 1 mM sodium phosphate, 1 mM sodium borate and 1 mM sodium citrate). The pH was altered by the addition of small amounts of 0.1 M HCl or 0.05 M NaOH. Peptide concentrations were in the range 0.5–1.0 mM.

reduced value for **1** compared with **3**, **5** and **6** is interesting and suggests altered dihedral propensities for the most helical pSer-containing peptide.

Discussion

An interesting feature of the TACC3–CHC binding interface in the crystal structure is that it does not exhibit the canonical recognition of phosphorylation, in which a cluster of basic residues on the binding partner clamps down on the phosphate group. Instead, the phosphorylated serine is positioned between two basic residues along one side of a helix in TACC3, and hydrophobic residues on another side of the helix line up to complement a groove on CHC. We hypothesized that the role of a phosphoserine in this arrangement is to
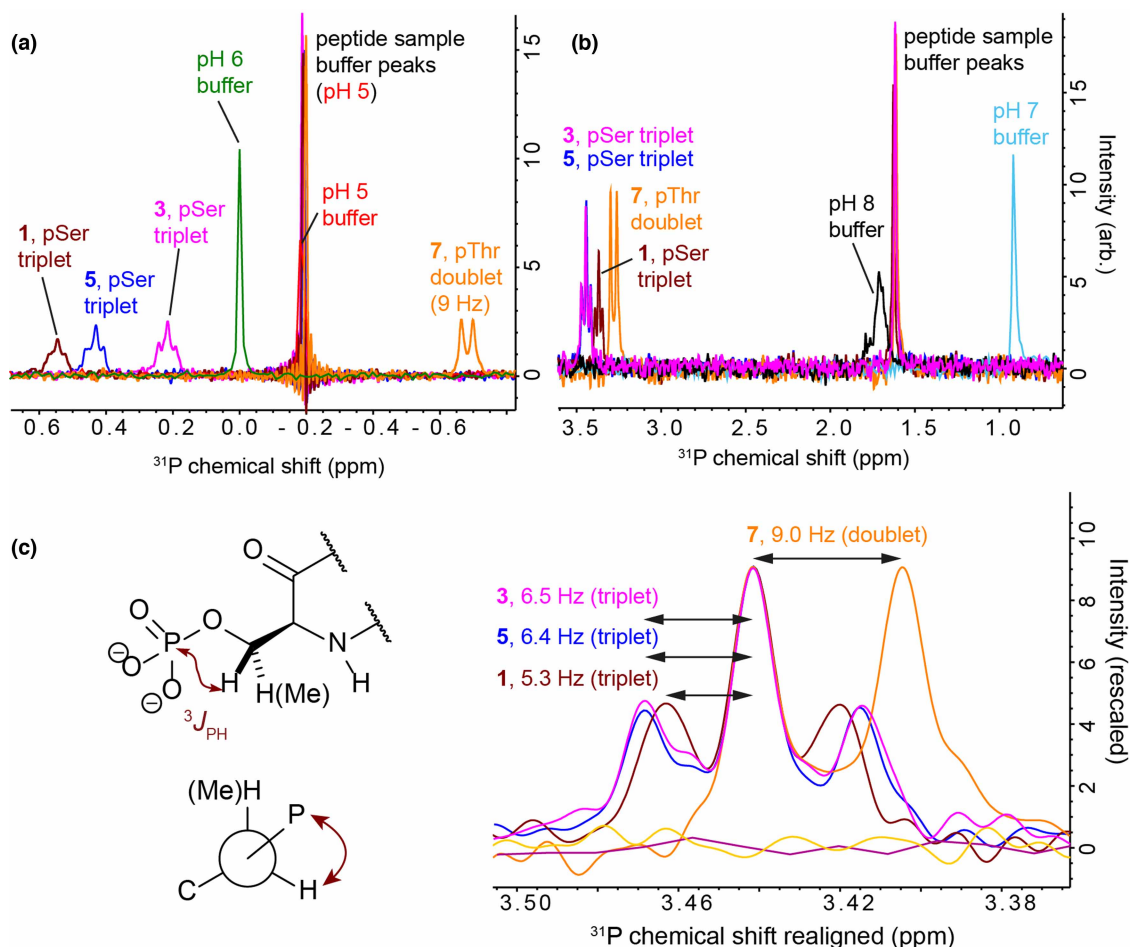
Figure 7. ³¹P NMR spectra for selected peptides (1, 3, 5, 6 and 7) and CD buffer standards at pH 5, 6, 7 and 8.
(**a**) At pH 5. (**b**) Just below pH 8. (**c**) Zoomed-in view of the peak fine-structure at pH ∼ 8 with spectra shown realigned to facilitate comparison. Spectra were recorded on a 600-MHz Bruker Avance spectrometer equipped with a quadruple resonance QCI-P cryoprobe at 5°C in CD buffer (10 mM NaCl, 1 mM sodium phosphate, 1 mM sodium borate and 1 mM sodium citrate). The pH was altered by the addition of small amounts of 0.1 M HCl or 0.05 M NaOH. Peptide concentrations were in the range 0.5–1.0 mM.

increase the helical propensity of this disordered region, and we set out to explore the conformational effects of phosphorylation in a model peptide system that is decoupled from intermolecular considerations. Here we have shown that phosphorylation of Ser residues stabilizes the α-helix in the context of an $Arg_{(i-3)}pSer_i Lys_{(i+4)}$ triad through charge-reinforced side chain interactions with positive co-operativity. This differs to other systems where multiple interactions between side chains are feasible, e.g. Glu–Lys–Glu which shows anti-cooperativity [38], and provides an exception to the general principle that internal phosphorylation is helix destabilizing [39]. Basic kinase-substrate motifs are common; an Arg at position −3 to the phosphorylated residue is a key selectivity determining residue within the recognition motif of 55 human protein kinases, including Aurora A and PKA [40], and there are over 2000 $Arg_{(i-3)}Ser_i Lys_{(i+4)}$ motifs in human proteins (identified using Expasy ScanProsite). In contrast, the corresponding Thr variants are not stabilized: Ser is slightly less helix destabilizing than Thr [4,5,11], whilst the latter favours a β-strand conformation [41] and branching at β-carbon is helix destabilizing [42]. These features likely reduce the number of side chain conformation pairs in which the pThr phosphoryl group is able to interact with the Arg and Lys while maintaining a helical structure (when compared with pSer). Moreover, recent studies have shown Thr phosphorylation promotes intraresidue hydrogen-bonding between the phosphate and the backbone amide, which would disrupt helix propagation in a manner analogous to the effect of Pro [27]. Taken together these results highlight the secondary structural sequence

context of phosphorylation and highlight the potential for it to affect PPIs not only through orthosteric [13] or allosteric [43] changes in recognition features and switching off recognition by changing conformation [14], but also through phospho-driven stabilization of an α-helical recognition motif.

Experimental procedures
Synthesis and purification of peptides

Amino acids were purchased from Novabiochem (Merck), Sigma–Aldrich or Fluorochem. All amino acids were N-Fmoc protected and side chains were protected with Boc (Lys), ^{t}Bu (Ser, Thr), Trt (Gln) or Pbf (Arg). Solvents and reagents used in peptide synthesis were sourced as follows: DMF and DCM (ACS grade) from Sigma–Aldrich; piperidine (99%) from Alfa Aesar; DIPEA (reagent grade) from Fluorochem; TFA (peptide grade) from Fluorochem; acetic anhydride (>99%) from Sigma–Aldrich; HCTU (reagent grade) from Fluorochem; formic acid (analytical reagent grade) from Fisher Scientific; *m*-Cresol (99%) from Acros Organics; thioanisole (99%) from Alfa Aesar; EDT (95%) from Sigma–Aldrich. Peptides were synthesized on Rink Amide MBHA resin by room temperature Fmoc-solid-phase peptide synthesis (SPPS) using the following cycle on an automated peptide synthesizer (CEM Liberty Blue). *Deprotection* — clean resin dip tube, wash with DMF (15 ml), add DMF: piperidine: formic acid (75 : 20 : 5) solution (6 ml), room temperature method (5 min), wash with DMF (15 ml), add DMF: piperidine: formic acid (75:20:5) solution (6 ml), room temperature method (5 min), wash with DMF (15 ml), clean resin dip tube, wash with DMF (15 ml). *Coupling* — add amino acid solution (0.2 M, 2.5 ml), add coupling reagent (HCTU; 0.2 M, 1 ml), add activator base (DIPEA; 0.2 M, 0.5 ml), room temperature method (18 min), wash with DMF (15 ml), drain. For double couplings, this step was repeated. N-*terminal acetylation* — after coupling of the final residue, the resin was ejected from the reaction vessel and N-terminal acetylation/cleavage and deprotection was performed manually. Acetic anhydride (10 *eq.*) and DIPEA (10 *eq.*) were dissolved in DMF (3 ml) and the solution was transferred to the resin. After 2 h, the resin was drained, washed with DMF (3 × 2 ml × 2 min) and successful capping determined by a negative colour test (Kaiser test) [44]. *Cleavage and deprotection* — the resin was washed with DMF, DCM and Et$_2$O (for each: 3 × 3 ml × 2 min). Peptides were then simultaneously cleaved and side chain deprotected with a prepared Reagent K cleavage cocktail (6 ml): TFA/m-cresol/H$_2$O/thioanisole/EDT (82.5/5/5/5/2.5). After 3 h, the resin was washed with fresh TFA (3 ml × 2 min) and the solution concentrated under a flow of N$_2$. The resulting oil was precipitated with ice-cold Et$_2$O (10 ml) and placed in a centrifuge (3000 rpm × 3 min). The supernatants were removed, the precipitate rinsed with ice-cold Et$_2$O (3 × 10 ml) and dried under a flow of N$_2$. *Purification* — peptides were purified by preparative HPLC using a Kinetex 5 μM EVO C18 preparative column (reversed phase) on an increasing gradient of acetonitrile to water (plus 0.1% TFA v/v in water) at a flow rate of 10 ml min^{-1}. Crude peptides were dissolved in minimal amounts of acetonitrile : water (1 : 1). Purification runs injected a maximum of 5 ml of crude peptide solution and were allowed to run for 35 min, with acetonitrile increasing from 5% to 95%, and the eluent scanned with a diode array at 210, 254 and 280 nm. Fractions were checked by LCMS, collected and lyophilized. Final purity of peptides was confirmed by high-resolution mass spectrometry and analytical HPLC (Supplementary Table S1).

Peptide solutions

'CD buffer' containing 1 mM sodium borate, 1 mM sodium citrate, 1 mM sodium phosphate and 10 mM NaCl, pH 7 [15], was used to facilitate easy alteration of peptide solution pH through the addition of small amounts of HCl or NaOH. This buffer has low absorbance in the region of wavelengths (190–260 nm) used for CD measurements. Solid lyophilized peptides were dissolved to give 1–2 mM solutions based on mass using CD buffer resulting in mildly acidic solutions (pH 6–7). Solution absorbance measurements at 280 nm were used to calculate more accurately the peptide concentration, based on a Tyr extinction coefficient of 1280 M^{-1} cm^{-1} [26,45], with 1 mM concentrations based on mass typically resulting in 0.7–1.0 mM solutions based on absorbance. Initial (∼1 ml) sample pH measurements were made using a three-point-calibrated meter equipped with a microelectrode probe. *In situ* pH measurements (e.g. during CD experiments) were made by careful removal of small volumes of sample to test with pH strips. *In situ* estimates of pH during NMR experiments were made using the buffer phosphate chemical shift by comparison with CD buffer-only samples calibrated at pH 5, 6, 7 and 8.

CD measurements

CD spectra were recorded using an APP Chirascan CD spectropolarimeter and 1 mm pathlength quartz cuvettes. Sample concentrations were typically 50–100 μM and once diluted to this degree had a pH matching the buffer alone (pH 7). Spectra were recorded at 5°C over wavelengths ranging from 260 to 180 nm, with data collected every 1 nm (1 nm s^{-1}), and each spectrum was recorded in duplicate. Temperature ramping experiments were recorded from 5 to 70–80°C with data recorded every ~1°C using a settling time between measurements of 120 s. A background spectrum for CD buffer alone was recorded for each data collection session, and background ellipticity values were subtracted from raw sample ellipticity values (θ) when calculating MREs using:

$$\text{MRE}(\lambda) = \frac{(\theta(\lambda) - \theta_{\text{buffer}}(\lambda)) \times M_w}{n \times \text{ pathlength (mm)} \times \text{ concentration (mg/ml)}}$$

where M_w is the peptide molecular weight, and n is the number of total peptide bonds, in each case taken to be 16 accounting for the acetyl capping group.

Several methods are available to estimate the helicity based on MRE values [46–48]. Estimates of peptide helicity were made using the relationship used by Baker et al. [49] as follows:

$$\% \text{ helix} = \frac{100 \times (\text{MRE}_{222} - \text{MRE}_{\text{coil}})}{-42500\left(1 - \left(\dfrac{3}{n}\right)\right)}$$

where MRE_{222} is the MRE value at 222 nm, $\text{MRE}_{\text{coil}} = 640 - 45T$ (with T in °C) = 415 deg cm^2 dmol^{-1} res^{-1} at 5°C and n is the number of backbone amide bonds including the N-terminal acetyl (as above). For a selection of peptides, MRE values were calculated from data collected over a wider (100×) range of concentrations (roughly 7–700 μM, Supplementary Figure S1). No change in MRE values was observed suggesting that peptide self-association does not occur.

Analysis of energetics

A simple estimate of the Gibbs free energy change (ΔG) of the helical (α) peptide in solution relative to its unfolded (u) state, can be calculated under a two-state, all-or-nothing approximation from the % helicity values determined experimentally by CD spectroscopy [11]. The equilibrium constant K_α between the folded and unfolded conformations in solution is defined by

$$K_\alpha = f_\alpha/(1 - f_\alpha)$$

where f_α is the fraction of helical and $(1 - f_\alpha) = f_u$, the fraction of unfolded peptide. The Gibbs free energy change on going from the unfolded state to the helical state is

$$\Delta G_x = -RT \ln(K_\alpha).$$

The change in the Gibbs free energy change on folding ($\Delta\Delta G$) is calculated, where appropriate, relative to the unphosphorylated peptide ($\Delta\Delta G = \Delta G_x - \Delta G_{\text{unphos}}$) or the equivalent motif Ala-control peptide ($\Delta\Delta G = \Delta G_x - \Delta G_{\mathbf{9/10}}$). $\Delta\Delta G$ values were also calculated relative also to the least helical pSer-containing peptide **3** ($\Delta\Delta G = \Delta G_x - \Delta G_{\mathbf{3}}$) to highlight how the introduction of potential sites for non-covalent interaction into the sequence influences conformational energetics; the $i + 5$ spacings in peptide **3** mean that it has no potential for inter-side chain interaction for a helical conformation.

NMR experiments

NMR spectra were recorded on a 600-MHz Bruker Avance spectrometer equipped with a quadruple resonance QCI-P cryoprobe, or a 950-MHz Bruker Ascend Aeon spectrometer equipped with a 5 mm TXO cryoprobe. For each peptide, natural abundance ^{1}H–^{15}N HMQC and ^{1}H–^{13}C HSQC (constant-time) spectra were recorded for 0.5–1.0 mM samples at 5°C. The low temperature maximizes the helical content of each peptide, and also (when combined with using pH between 6 and 7) slows proton exchange enough to allow the Arg Hε–Nε

correlation to be visible. Clean spectra ^{1}H–^{15}N HMQC took ~12 h to record. To reduce experiment time (to ~6 h), ^{1}H–^{13}C HSQC spectra were recorded with reduced spectral width in ^{13}C (typically 20 ppm centred on 56 ppm), and the spectrum folded out to show the position of the non-Hα–Cα correlations. ^{1}H–^{1}H TOCSY and ^{1}H–^{1}H NOESY spectra were recorded and used to assign resonances for each peptide through residue-specific shifts and strong $(i, i-1)$ NOE connectivity. Spectra were initially processed using NMRPipe/NMRDraw [50], and resonance assignments were carried out using CCPNmr Analysis [51]. Systematic patterns of peak shifts in spectra for different but related peptides were used to aid assignment. Full assignment of backbone resonances was possible (with the exception of uncharacterized amide carbonyl carbons). ^{13}C resonance assignment in ^{1}H–^{13}C HSQC spectra required a unique attached ^{1}H resonance and/or the peak position to occur in a residue-specific region of the spectrum. In a few instances, Ala Cα and Cβ resonances could not be independently assigned so two positions — marking the potential range in Cα/Cβ shift — were recorded. Secondary shifts $(\Delta\delta)$ = observed shifts (δ) — expected shifts for that residue in a random coil conformation (δ_{RC}), were calculated using recently published δ_{RC} values for phosphorylated residues [34] available via the website:

(https://www1.bio.ku.dk/english/research/bms/sbinlab/randomchemicalshifts2/). 1D ^{31}P spectra were recorded on the 600-MHz spectrometer using the 30° flip angle pulse sequence.

Analysis of Arg$_{(i-3)}$Ser$_i$ Lys$_{(i+4)}$ motifs in human proteome

A search for Arg$_{(i-3)}$Ser$_i$ Lys$_{(i+4)}$ motifs in human proteins was carried out using the Expasy ScanProsite tool (https://prosite.expasy.org/scanprosite/) using the motif pattern 'R-{P}(2)-S-{P}(3)-K', excluding isoforms, and filtering to taxonomy 'Homo sapiens'. This generated 2226 hits in 1966 sequences, based on release 2021_04 of 29-Sep-21: 565 928entries) of the UniProtKB/Swiss-Prot database.

Data Availability

The authors declare that the main data supporting the findings of this study are available within the article and its Supplementary materials. Raw data were generated at the University of Leeds and CD datasets and NMR chemical shift lists are available in the University of Leeds Data Repository via the DOI: 10.5518/1104.

Competing Interests

The authors declare that there are no competing interests associated with the manuscript.

CRediT Author Contribution

Richard Bayliss: Conceptualization, supervision, funding acquisition, writing — review and editing. **Matthew Batchelor**: Investigation, writing — original draft. **Robert S. Dawber**: Investigation, writing — original draft. **Andrew J. Wilson**: Conceptualization, supervision, funding acquisition, writing — review and editing.

Abbreviations

CD, circular dichroism; CHC, clathrin heavy chain; MREs, mean residue ellipticities; PPIs, protein–protein interactions; SPPS, solid-phase peptide synthesis; TACC, transforming acidic coiled coil.

References

1   Bullock, B.N., Jochim, A.L. and Arora, P.S. (2011) Assessing helical protein interfaces for inhibitor design. *J. Am. Chem. Soc.* **133**, 14220–14223 https://doi.org/10.1021/ja206074j

2   Wang, H., Dawber, R.S., Zhang, P., Walko, M., Wilson, A.J. and Wang, X. (2021) Peptide-based inhibitors of protein–protein interactions: biophysical, structural and cellular consequences of introducing a constraint. *Chem. Sci.* **12**, 5977–5993 https://doi.org/10.1039/D1SC00165E

3   Muttenthaler, M., King, G.F., Adams, D.J. and Alewood, P.F. (2021). Trends in peptide drug discovery. *Nat. Rev. Drug Discov.* **20**, 309–325 https://doi.org/10.1038/s41573-020-00135-8

4   Nick Pace, C. and Martin Scholtz, J. (1998) A helix propensity scale based on experimental studies of peptides and proteins. *Biophys. J.* **75**, 422–427 https://doi.org/10.1016/S0006-3495(98)77529-0

5   Miller, S.E., Watkins, A.M., Kallenbach, N.R. and Arora, P.S. (2014) Effects of side chains in helix nucleation differ from helix propagation. *Proc. Natl Acad. Sci. U.S.A.* **111**, 6636–6641 https://doi.org/10.1073/pnas.1322833111

6   Doig, A.J., Chakrabartty, A., Klingler, T.M. and Baldwin, R.L. (1994) Determination of free energies of N-capping in α-helixes by modification of the Lifson-Roig helix-coil theory to include N- and C-capping. *Biochemistry* **33**, 3396–3403 https://doi.org/10.1021/bi00177a033

7   Aurora, R. and Rosee, G.D. (1998) Helix capping. *Protein Sci.* **7**, 21–38 https://doi.org/10.1002/pro.5560070103

8   Shi, Z.S., Olson, C.A. and Kallenbach, N.R. (2002) Cation-π interaction in model α-helical peptides. *J. Am. Chem. Soc.* **124**, 3284–3291 https://doi.org/10.1021/ja0174938

9   Olson, C.A., Shi, Z.S. and Kallenbach, N.R. (2001) Polar interactions with aromatic side chains in α-Helical peptides: Ch⋯O H-Bonding and cation−π Interactions. *J. Am. Chem. Soc.* **123**, 6451–6452 https://doi.org/10.1021/ja015590v

10   Tsou, L.K., Tatko, C.D. and Waters, M.L. (2002) Simple cation–π interaction between a phenyl ring and a protonated amine stabilizes an α-helix in water. *J. Am. Chem. Soc.* **124**, 14917–14921 https://doi.org/10.1021/ja026721a

11   Lyu, P., Liff, M., Marky, L. and Kallenbach, N. (1990) Side chain contributions to the stability of alpha-helical structure in peptides. *Science* **250**, 669–673 https://doi.org/10.1126/science.2237416

12   Iakoucheva, L.M., Radivojac, P., Brown, C.J., O'Connor, T.R., Sikes, J.G., Obradovic, Z. et al. (2004) The importance of intrinsic disorder for protein phosphorylation. *Nucleic Acids Res.* **32**, 1037–1049 https://doi.org/10.1093/nar/gkh253

13   Nishi, H., Hashimoto, K. and Panchenko, A.R. (2011) Phosphorylation in protein–protein binding: effect on stability and function. *Structure* **19**, 1807–1815 https://doi.org/10.1016/j.str.2011.09.021

14   Bah, A., Vernon, R.M., Siddiqui, Z., Krzeminski, M., Muhandiram, R., Zhao, C. et al. (2015) Folding of an intrinsically disordered protein by phosphorylation as a regulatory switch. *Nature* **519**, 106–109 https://doi.org/10.1038/nature13999

15   Errington, N. and Doig, A.J. (2005) A phosphoserine–lysine salt bridge within an α-helical peptide, the strongest α-helix side-chain interaction measured to date. *Biochemistry* **44**, 7553–7558 https://doi.org/10.1021/bi050297j

16   Andrew, C.D., Warwicker, J., Jones, G.R. and Doig, A.J. (2002) Effect of phosphorylation on α-helix stability as a function of position. *Biochemistry* **41**, 1897–1905 https://doi.org/10.1021/bi0113216

17   Elbaum, M.B. and Zondlo, N.J. (2014) OGlcNAcylation and phosphorylation have similar structural effects in α-helices: post-translational modifications as inducible start and stop signals in α-helices, with greater structural effects on threonine modification. *Biochemistry* **53**, 2242–2260 https://doi.org/10.1021/bi500117c

18   Szilák, L., Moitra, J. and Vinson, C. (1997) Design of a leucine zipper coiled coil stabilized 1.4 kcal mol^{-1} by phosphorylation of a serine in the e position. *Protein Sci.* **6**, 1273–1283 https://doi.org/10.1002/pro.5560060615

19   Signarvic, R.S. and DeGrado, W.F. (2003) De novo design of a molecular switch: phosphorylation-dependent association of designed peptides. *J. Mol. Biol.* **334**, 1–12 https://doi.org/10.1016/j.jmb.2003.09.041

20   Kumar, A., Gopalswamy, M., Wolf, A., Brockwell, D.J., Hatzfeld, M. and Balbach, J. (2018) Phosphorylation-induced unfolding regulates p19INK4d during the human cell cycle. *Proc. Nat Acad. Sci. U.S.A.* **115**, 3344–3349 https://doi.org/10.1073/pnas.1719774115

21   Harrington, L., Fletcher, J.M., Heermann, T., Woolfson, D.N. and Schwille, P. (2021) De novo design of a reversible phosphorylation-dependent switch for membrane targeting. *Nat. Commun.* **12**, 1472 https://doi.org/10.1038/s41467-021-21622-5

22   Burgess, S.G., Mukherjee, M., Sabir, S., Joseph, N., Gutiérrez-Caballero, C., Richards, M.W. et al. (2018) Mitotic spindle association of TACC3 requires Aurora-A-dependent stabilization of a cryptic α-helix. *EMBO J.* **37**, e97902 https://doi.org/10.15252/embj.201797902

23   Scholtz, J.M., York, E.J., Stewart, J.M. and Baldwin, R.L. (1991) A neutral, water-soluble, α-helical peptide: the effect of ionic strength on the helix-coil equilibrium. *J. Am. Chem. Soc.* **113**, 5102–5104 https://doi.org/10.1021/ja00013a079

24   Shalongo, W., Dugad, L. and Stellwagen, E. (1994) Distribution of helicity within the model peptide Acetyl(AAQAA)3amide. *J. Am. Chem. Soc.* **116**, 8288–8293 https://doi.org/10.1021/ja00097a039

25   Huyghues-Despointes, B.M.P., Martin Scholtz, J. and Baldwin, R.L. (1993) Helical peptides with three pairs of Asp–Arg and Glu–Arg residues in different orientations and spacings. *Protein Sci.* **2**, 80–85 https://doi.org/10.1002/pro.5560020108

26   Greenfield, N.J. (2006) Using circular dichroism spectra to estimate protein secondary structure. *Nat. Protoc.* **1**, 2876–2890 https://doi.org/10.1038/nprot.2006.202

27   Pandey, A.K., Ganguly, H.K., Sinha, S.K., Daniels, K.E., Yap, G.P.A., Patel, S. et al. (2020) An inherent structural difference between serine and threonine phosphorylation: phosphothreonine prefers an ordered, compact, cyclic conformation. *bioRxiv* 2020.2002.2029.971382

28   Scholtz, J.M., Qian, H., Robbins, V.H. and Baldwin, R.L. (1993) The energetics of ion-pair and hydrogen-bonding interactions in a helical peptide. *Biochemistry* **32**, 9668–9676 https://doi.org/10.1021/bi00088a019

29   Smith, J.S. and Scholtz, J.M. (1998) Energetics of polar side-chain interactions in helical peptides: salt effects on ion pairs and hydrogen bonds. *Biochemistry* **37**, 33–40 https://doi.org/10.1021/bi972026h

30   Selenko, P., Frueh, D.P., Elsaesser, S.J., Haas, W., Gygi, S.P. and Wagner, G. (2008) In situ observation of protein phosphorylation by high-resolution NMR spectroscopy. *Nat. Struct. Mol. Biol.* **15**, 321–329 https://doi.org/10.1038/nsmb.1395

31   Wishart, D.S., Sykes, B.D. and Richards, F.M. (1991) Relationship between nuclear magnetic resonance chemical shift and protein secondary structure. *J. Mol. Biol.* **222**, 311–333 https://doi.org/10.1016/0022-2836(91)90214-Q

32   Wishart, D.S. and Sykes, B.D. (1994) The ^{13}C Chemical-Shift Index: A simple method for the identification of protein secondary structure using ^{13}C chemical-shift data. *J. Biomol. NMR* **4**, 171–180 https://doi.org/10.1007/BF00175245

33   Wishart, D.S., Sykes, B.D. and Richards, F.M. (1992) The chemical shift index: a fast and simple method for the assignment of protein secondary structure through NMR spectroscopy. *Biochemistry* **31**, 1647–1651 https://doi.org/10.1021/bi00121a010

34 Hendus-Altenburger, R., Fernandes, C.B., Bugge, K., Kunze, M.B.A., Boomsma, W. and Kragelund, B.B. (2019) Random coil chemical shifts for serine, threonine and tyrosine phosphorylation over a broad pH range. *J. Biomol. NMR* **73**, 713–725 https://doi.org/10.1007/s10858-019-00283-z

35 Pascal, S.M., Yamazaki, T., Singer, A.U., Kay, L.E. and Forman-Kay, J.D. (1995) Structural and dynamic characterization of the phosphotyrosine binding region of an Src homology 2 domain–phosphopeptide complex by NMR relaxation, proton exchange, and chemical shift approaches. *Biochemistry* **34**, 11353–11362 https://doi.org/10.1021/bi00036a008

36 Batchelor, M., Wolny, M., Baker, E.G. Paci, E., Kalverda, A.P. and Peckham, M. (2019) Dynamic ion pair behavior stabilizes single α-helices in proteins. *J. Biol. Chem.* **294**, 3219–3234 https://doi.org/10.1074/jbc.RA118.006752

37 Zandarashvili, L., Esadze, A. and Iwahara, J. (2013) NMR studies on the dynamics of hydrogen bonds and ion pairs involving lysine side chains of proteins. In *Advances in Protein Chemistry and Structural Biology* (Christov, C.Z. ed.), vol. **93**, pp. 37–80, Academic Press, Oxford, UK

38 Iqbalsyah, T.M. and Doig, A.J. (2005) Anticooperativity in a Glu–Lys–Glu salt bridge triplet in an isolated α-helical peptide. *Biochemistry* **44**, 10449–10456 https://doi.org/10.1021/bi0508690

39 Szilák, L., Moitra, J., Krylov, D. and Vinson, C. (1997) Phosphorylation destabilizes α-helices. *Nat. Struct. Biol.* **4**, 112–114 https://doi.org/10.1038/nsb0297-112

40 Bradley, D., Vieitez, C., Rajeeve, V., Selkrig, J., Cutillas, P.R. and Beltrao, P. (2021) Sequence and structure-based analysis of specificity determinants in eukaryotic protein kinases. *Cell Rep.* **34**, 108602 https://doi.org/10.1016/j.celrep.2020.108602

41 Minor, D.L. and Kim, P.S. (1994) Measurement of the β-sheet-forming propensities of amino acids. *Nature* **367**, 660–663 https://doi.org/10.1038/367660a0

42 Lyu, P.C., Sherman, J.C., Chen, A. and Kallenbach, N.R. (1991) Alpha-helix stabilization by natural and unnatural amino acids with alkyl side chains. *Proc. Natl Acad. Sci. U.S.A.* **88**, 5317–5320 https://doi.org/10.1073/pnas.88.12.5317

43 Skinner, J.J., Wang, S., Lee, J., Ong, C., Sommese, R., Sivaramakrishnan, S. et al. (2017) Conserved salt-bridge competition triggered by phosphorylation regulates the protein interactome. *Proc. Natl Acad. Sci. U.S.A.* **114**, 13453–13458 https://doi.org/10.1073/pnas.1711543114

44 Kaiser, E., Colescott, R.L., Bossinger, C.D. and Cook, P.I. (1970) Color test for detection of free terminal amino groups in the solid-phase synthesis of peptides. *Anal. Biochem.* **34**, 595–598 https://doi.org/10.1016/0003-2697(70)90146-6

45 Kelly, S.M., Jess, T.J. and Price, N.C. (2005) How to study proteins by circular dichroism. *Biochim. Biophys. Acta - Proteins Proteom.* **1751**, 119–139 https://doi.org/10.1016/j.bbapap.2005.06.005

46 Lacroix, E., Viguera, A.R. and Serrano, L. (1998) Elucidating the folding problem of α-helices: local motifs, long-range electrostatics, ionic-strength dependence and prediction of NMR parameters. *J. Mol. Biol.* **284**, 173–191 https://doi.org/10.1006/jmbi.1998.2145

47 Sommese, R.F., Sivaramakrishnan, S., Baldwin, R.L. and Spudich, J.A. (2010) Helicity of short E-R/K peptides. *Protein Sci.* **19**, 2001–2005 https://doi.org/10.1002/pro.469

48 Shepherd, N.E., Hoang, H.N., Abbenante, G. and Fairlie, D.P. (2005) Single turn peptide alpha helices with exceptional stability in water. *J. Am. Chem. Soc.* **127**, 2974–2983 https://doi.org/10.1021/ja0456003

49 Baker, E.G. Bartlett, G.J., Crump, M.P., Sessions, R.B., Linden, N., Faul, C.F.J. et al. (2015). Local and macroscopic electrostatic interactions in single α-helices. *Nat. Chem. Biol.* **11**, 221–228 https://doi.org/10.1038/nchembio.1739

50 Delaglio, F., Grzesiek, S., Vuister, G.W., Zhu, G., Pfeifer, J. and Bax, A. (1995). NMRPipe: A multidimensional spectral processing system based on UNIX pipes. *J. Biomol. NMR* **6**, 277–293 https://doi.org/10.1007/BF00197809

51 Vranken, W.F., Boucher, W., Stevens, T.J., Fogh, R.H., Pajon, A., Llinas, M. et al. (2005) The CCPN data model for NMR spectroscopy: Development of a software pipeline. *Proteins* **59**, 687–696 https://doi.org/10.1002/prot.20449